Kernel-Based Reconstruction of C-11-Hydroxyephedrine Cardiac PET Images of the Sympathetic Nervous System

Zahra Ashouri, Chad R. Hunter, Benjamin A. Spencer, Guobao Wang, Richard M. Dansereau and Robert A. deKemp

***Abstract*— Image reconstruction for positron emission tomography (PET) can be challenging and the resulting image typically has high noise. The kernel-based reconstruction method [1], incorporates prior anatomic information in the reconstruction algorithm to reduce noise while preserving resolution. Prior information is incorporated in the reconstruction algorithm by means of spatial kernels originally used in machine learning. In this paper, the kernel-based method is used to reconstruct PET images of sympathetic innervation in the heart. The resulting images are compared with standard Ordered Subset Expectation Maximization (OSEM) reconstructed images qualitatively and quantitatively using data from 6 human subjects. The kernel-based method demonstrated superior SNR with preserved contrast and accuracy compared to OSEM.**

I. Introduction

Positron emission tomography (PET) is a medical imaging tool that is used to observe metabolic processes in the body using radioactive tracers. Although PET is a powerful imaging method to quantify the biochemical processes of different tissues and organs, it has limited accuracy due to detector resolution and statistical noise. Several methods have been proposed to increase PET image quality. However, if these effects can be accurately modeled during reconstruction, further post-processing might be avoided and could reduce bias in the final resulting image. One technique for increasing reconstructed image quality is to use prior information [2]. Prior information can be incorporated in the form of a regularization function [3]. Anatomical information from other image modalities such as computed tomography (CT) or magnetic resonance imaging (MRI) can be used as prior anatomical information. There are a few different methods which use anatomical information as a prior for image reconstruction. Nguyen et al have proposed a non-local means (NLM) approach [4]. In this method, a PET image is adaptively smoothed with a weight matrix. Weights are derived to reflect self-similarity in PET images by means of information provided by the anatomical image. One of the most common approaches to reconstruct PET images is to use maximum likelihood expectation maximization (MLEM) [5]. This method comes from the probability density function in PET and is a straight forward iterative update. The convergence of MLEM is slow, but can be accelerated using Ordered Subset Expectation Maximization (OSEM) [6]. Although OSEM might not converge to the true maximum likelihood (ML) solution, it reduces the processing time proportional to the number of subsets, and with post-reconstruction filtering the reconstructed images can have excellent quality. Therefore, OSEM is the method used in most clinical settings [3].

Wang et al incorporated prior information in a form of an image feature space [1]. Image intensity for each pixel of a PET image is a function of a set of features where the features are derived from prior information. This function is defined using a kernel method and is assumed to be linear in kernel space. The results of the kernel-based method were investigated using a Zubal head phantom and also real patient data for head scans, and is was shown that it was superior to standard OSEM. In this paper, we apply this method to dynamic patient scans of the heart. This is different from the head scan study, since the chest contains involuntary motion, but the head does not. For instance, images of the heart are affected by both cardiac and respiratory motion which is always present and because of it, high quality PET images are harder to achieve; whereas the position of the head can be fixed. This paper is organized as follows: in section II, iterative and kernel-based PET image reconstruction is defined; section III explains the evaluation procedure and the two methods are compared in section IV; section V is the discussion and conclusion.

II. Theory

A. Iterative Reconstruction for PET

PET images represent the detection of high energy photon pairs produced through annihilation of positrons emitted from a radioactive tracer. Using radiation detectors, these photons are measured. The probability of measuring events follows a Poisson distribution. The Expectation Maximization (EM) algorithm maximizes the log-likelihood function and therefore helps to find the maximum likelihood estimate of image x. The result is an iterative update of the image [2].

$$x^{n+1} = \frac{x^n}{P^T.\ \mathbf{1}_M}.\left(P^T \frac{y}{Px^n + r}\right) \quad (1)$$

* Research supported by Natural Sciences and Engineering Research Council (NSERC) of Canada.

Zahra Ashouri is with the Ottawa Heart Institute and Carleton University. e-mail: zashouritalouki@ottawaheart.ca).

Chad Hunter is a post doc with the Ottawa Heart Institute. (e-mail: CHunter@ottawaheart.ca).

Benjamin A. Spencer is a post doc at UC Davis medical center. (email: benspencer@ucdavis.edu).

Guobao Wang is an assistant professor with the Department of Radiology, UC Davis. (e-mail: gbwang@ucdavic.edu).

Richard M. Dansereau is with the Department of Systems and Computer Engineering, Carleton University (e-mail: rdanse@sce.carleton.ca).

Robert DeKemp is with the Ottawa Heart Institute and Ottawa University (e-mail: radekemp@ottawaheart.ca).

978-1-5386-1311-5/19/$31.00 ©2019 IEEE

Where: y is the projection data and $P \in R^{M\times N}$(N number of voxels), is the detection probability matrix. The unknown emission image x, is related to r and defined as the expectation of random and scatter events, as shown below:

$$\bar{y} = Px + r \tag{2}$$

B. PET Image Reconstruction using Kernel in EM

For kernel-based expectation maximization (KEM), PET image reconstruction is accomplished by the use of kernels derived from machine learning methods [1]. For this method, a feature vector f_j is identified for pixel intensity x_j, and can be defined by a linear combination of feature vectors of the neighboring pixels. As shown in (3), this will form the kernel space.

$$x_j = \sum_{l=1}^{N} \alpha_l \kappa(f_j, f_l) \tag{3}$$

Where α, is the kernel coefficient and $\kappa(f_j, f_l)$ identifies the similarity of feature, between pixel x_j and pixel x_l in its neighborhood. Equation (3) can be written in matrix form as

$$x = K\alpha. \tag{4}$$

Where elements of matrix K are given by $\kappa(f_j, f_l)$ for the (j, l)th element. Different kernels can be used such as the Gaussian or polynomial kernel. Here, the radial Gaussian kernel has been used. The KEM method of reconstruction is derived by substituting (4) in (2). The iterative solution would be updated to:

$$\alpha^{n+1} = \frac{\alpha^n}{K^T P^T 1_M} . \left(K^T P^T \frac{y}{PK\alpha^n + r} \right) \tag{5}$$

This iterative algorithm can be solved using OSEM with the kernel embedded in the iterative update.

C. Kernel Reconstruction

To generate the prior image in the kernel-based method, composite frames are made by summing multiple time frames from the dynamic image series. This helps to preserve spatial information apparent in most frames at the expense of losing temporal information. Wang et al have tested different numbers of composite frames and concluded that for their problem three composite frames worked best [1]. A compromise is needed in selecting the number of composite frames. A large number will result in high noise in the composite frames and a small number will make the kernel ineffective. Composite frames should preserve the image contrast and reduce the noise at the same time. We used three composite frames, the first frame describes the blood input, the second encompasses the transitional phase of the tracer and the final frame describes the uptake in important organs and tissues. These composite frames are then reconstructed using the standard OSEM algorithm. This is a fast reconstruction as there are only three frames. From these reconstructed frames, the features for building the kernel matrix are extracted. The feature vector is the average of the reconstructed composite frames for each pixel. Matrix K, is constructed by comparing the feature vectors for a pixel with all the feature vectors of its neighboring pixels. A cubic window centered on a pixel of interest defines where the neighboring pixels are located. A radial Gaussian filter is used to calculate the weights on the neighboring pixels. The size of the neighborhood is chosen to be $7 \times 7 \times 7$ and the Gaussian parameter (σ) is 1 in this study. To further sparsify the kernel the 50 highest weight values in the neighborhood are selected to contributed to the matrix and the rest are set to zero.

III. Method

To evaluate the KEM method, the reconstructed images are compared to OSEM reconstruction. For this comparison the left ventricle, liver and a region inside the left ventricle blood cavity are chosen. The left ventricle is segmented using our clinical in-house developed software called FlowQuant™. First, the images reconstructed using OSEM were segmented, then the same mask is mapped to KEM and also OSEM with various post-filtering. Kinetic modelling was achieved using a one-tissue compartment model. Compartment models are a way of mathematical modeling biological processes. In this paper, the compartment model will explain tracer absorption and distribution in body organs. The one compartment model assumes a homogeneous distribution throughout the volume of blood or tissue and that the decay rate of the tracer in the organ is constant [7]. The output of left ventricle segmentation is the signal we are looking at; now we need to calculate background noise to be able to calculate SNR. For this goal, an area inside the blood cavity of the left ventricle is chosen manually. We expect this area to be homogeneous and therefore to have low standard deviation in reconstructed pixel intensities. This standard deviation is considered as noise. Liver is also expected to be homogeneous; therefore, a manually selected area in the liver is defined and standard deviation and mean values in this region is calculated. We used real patient data and therefore there is no ground-truth or gold standard. With no gold standard in hand, SNR and contrast are defined in equations (6) and (7) with the signal value in the left ventricle and noise calculated in the blood cavity. In these equations, "LV" is defined as the left ventricle wall and "Blc" is the blood cavity in a region inside the left ventricle. To show

$$SNR = \frac{Mean(LV)}{std(Blc)} \tag{6}$$

$$Contrast = \frac{mean(LV) - mean(Blc)}{mean(LV)} \tag{7}$$

The study population includes dynamic PET imaging acquired from 6 patients with C-11-hydroxyephedrine (HED) tracer. The HED tracer is widely used for myocardium neuronal imaging and has an isotope half-life of 20 min. The scans are acquired by GE D600 PET/CT scanner. The scan time was 60 min split into 25 time frames defined as follows: 9×10s, 3×30s, 2×60s, and 11×300s. Final reconstructed images had 47 axial slices of the heart region. These frames are split to three 20 min length composite frames by summing the frames in 20 minute consecutive intervals, and then from this the kernel is produced. This kernel is then used to reconstruct all dynamic frames. SNR, contrast and LV activity were compared between OSEM and KEM using paired sampled T-test [8] with $P < 0.05$ considered as significant.

IV. Results

In fig. 1. SNR versus contrast is shown. The values presented in this figure were averaged over the last four uptake frames. In our analysis, we have focused on the later frames or uptake frames where the tracer uptake is largely in heart tissue. Later in fig. 3 we will show the values for each frame separately. For fig. 1 the level of post-reconstruction smoothing is accomplished with a gaussian spatial filter set to a specific full width half maximum (FWHM). We can see that by increasing the level of post-reconstruction filtering for OSEM, the SNR initially increases as the contrast decreases.

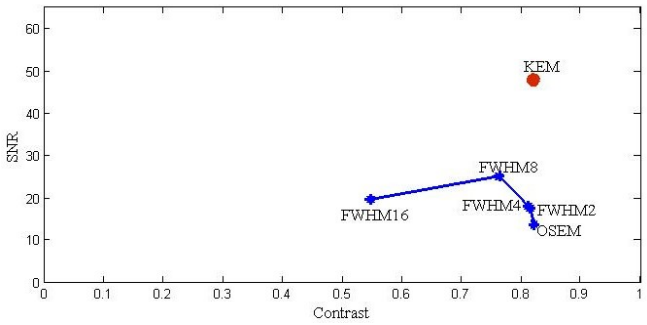

Figure 1: SNR versus contrast for OSEM with different smoothing filters and KEM.

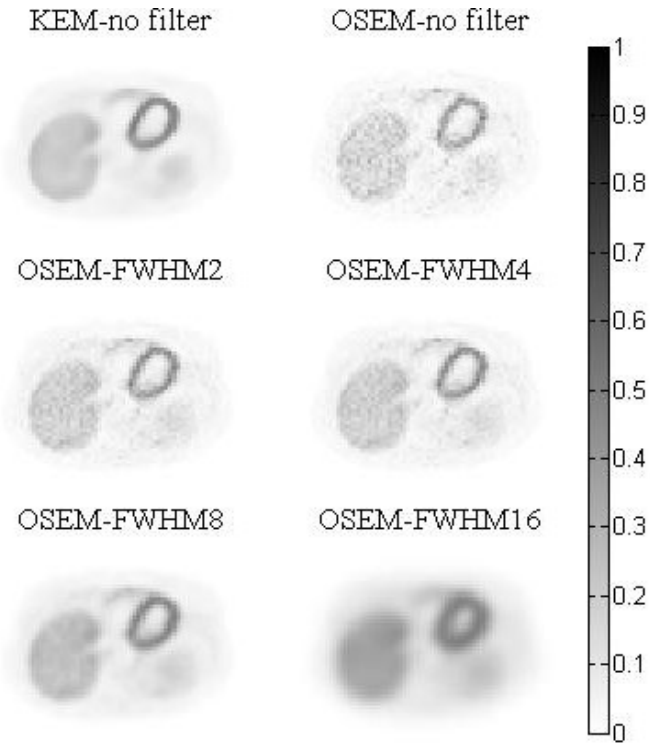

Figure 2. Transaxial slice of the last frame from one of the patients comparing KEM reconstruction with OSEM reconstruction using different levels of post filtering.

After reaching certain level of post-reconstruction filtering, the SNR decreases with further increased filtering. However, KEM produces a high SNR without a significant impact on contrast. From fig. 1, we can choose the post filtering which gives the highest SNR among others with no significant reduction in contrast and compare it with KEM. FWHM = 4 mm (herein called FWHM4) seems to satisfy these conditions and is therefore chosen for the rest of the comparisons.

Fig. 2 shows a transaxial slice of the heart in the last frame for one of the patients showing the results of KEM and OSEM with different levels of post filtering. As greater post-reconstruction smoothing is used the image resolution and contrast both suffer and therefore the quality degrades.

SNR and contrast values averaged over all patients in each frame are shown in fig. 3. The first two dynamic frames are excluded since the activity in those frames was very low and it caused the standard deviation and mean value at these frames to be negligible, thus leading to an unreliable SNR and contrast value. In addition, this shows that the SNR is much higher in KEM than OSEM, even with optimal post-reconstruction filtering.

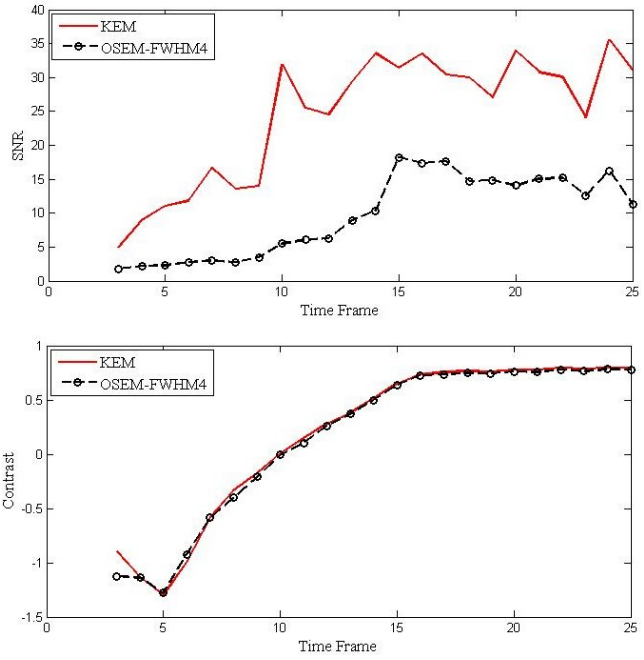

Figure 3. Average SNR and contrast for all the patients for KEM and OSEM with 4mm post filtering.

The mean and standard deviation values in different tissue types (blood cavity, heart and liver) for OSEM with 4 mm post filtering and KEM are presented in fig. 4. As expected, KEM does not change the mean value in the tissues of interest but decreases the standard deviation mainly due to reduced noise. The standard deviation in the left ventricle does not change significantly since it is a small structure with high counts and therefore does not contain as much noise.

The uptake polar maps for one normal and one ischemic patient are shown in fig. 5, in the units of kBq/cc, which shows that KEM does not change the uptake mean values in the left ventricle. In this figure "S" corresponds to septal wall, "L" is the lateral wall and "P" represents the posterior wall of the left ventricle.

For a statistical comparison, we have combined all the normalized polar map segmental values from KEM and

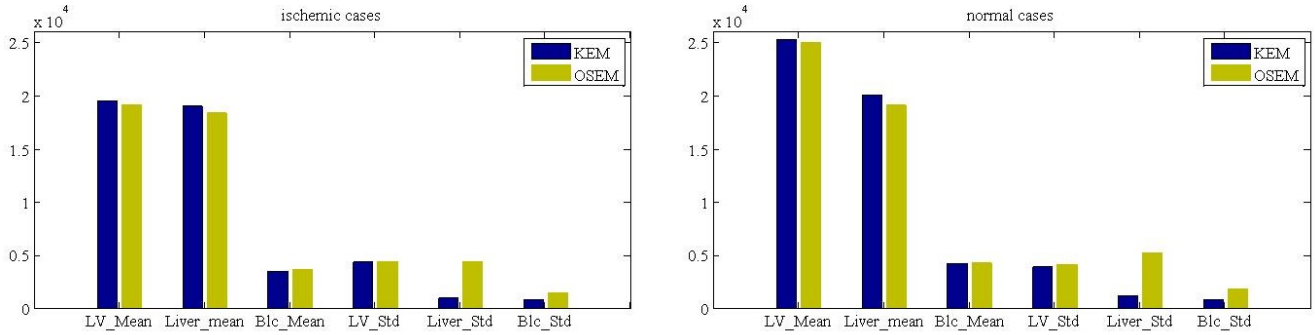

Figure. 4: Mean and standard deviation (Std) of late uptake values in different tissue regions for the normal subjects (right) and ischemic patients (left). LV is the left ventricle, Blc is the blood cavity region in the left ventricle. Liver and blood Std was significantly reduced using KEM compared to OSEM.

compared it to OSEM using paired T-test [8]. The mean value of the normalized segmented regions is 83.41 for KEM and 83.64 for OSEM and the *P* value is 0.035. This P value indicates that there is a significant difference between two data sets; but the absolute difference of mean values is very small (0.25%).

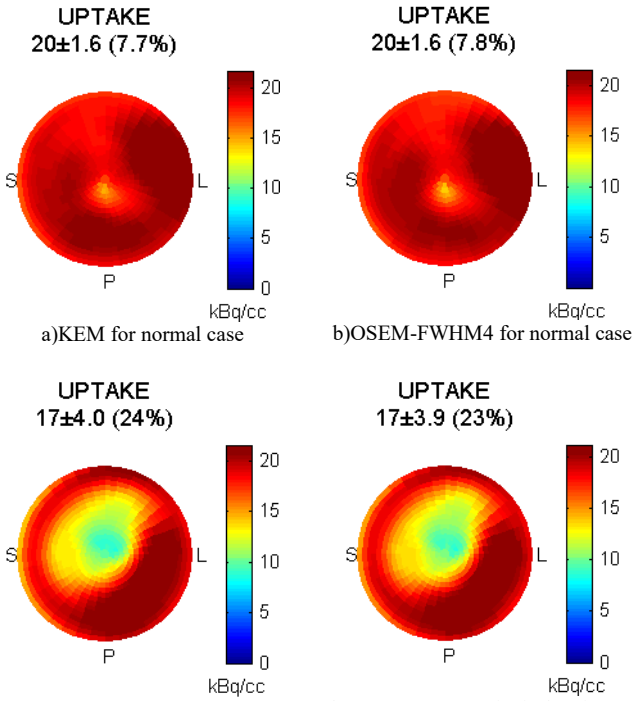

a)KEM for normal case b)OSEM-FWHM4 for normal case

c)KEM for ischemic case d)OSEM-FWHM4 for ischemic case

Figure 5. Polar map of the left ventricle distribution in the uptake frames

V. Conclusion

KEM PET image reconstruction was compared to OSEM for cardiac images of C-11-HED uptake. Our results shows that the kernel-based method can improve SNR for different frames while keeping the contrast high. It should be noted that because of the way the kernel is constructed, it might miss small objects and thus result in low resolution on small objects. There is a tradeoff between SNR and resolution and depending on the application clinicians should decide if the loss in resolution is worth the gain in SNR. Future work will involve optimization of this trade off by experimentation on the kernel to try to preserve the resolution in small targets.

References

[1] G. Wang and J. Qi. "Pet image reconstruction using kernel method," *IEEE Transactions on Medical Imaging*, vol. 34, no. 1, pp. 61–71, 2015.

[2] J. Qi and R. M. Leahy, "Iterative reconstruction techniques in emission computed tomography," *Physics in Medicine and Biology*, vol. 51, no. 15, pp. R541–R578, 2006.

[3] B. Bai, Q. Li, and R. M. Leahy, "Magnetic resonance-guided positron emission tomography image reconstruction," *Seminars in Nuclear Medicine,* vol. 43, pp. 30–44, 2013.

[4] V.-G. Nguyen and S.-J. Lee, "Nonlocal-means approaches to anatomy-based PET image reconstruction," *Proc. IEEE Nuclear. Science Symposium*, pp. 3273–3277, 2010.

[5] L. A. Shepp, Y. Vardi, "Maximum likelihood reconstruction for emission tomography," *IEEE Transaction on Medical* Imag*ing*, vol. 1, no. 2, pp. 113-22, 1982.

[6] H. M. Hudson, R. S. Larkin, "Accelerated image reconstruction using ordered subsets of projection data," *IEEE Transaction Medical* Imag*ing*, vol. 13, pp. 601-609, 1994.

[7] H. Watabe, Y. Ikoma, Y. Kimura, M. Naganawa, M. Shidahara, "PET kinetic analysis-compartmental model," *Annals of Nuclear Medicine*, vol. 20, pp. 583-588, 2006.

[8] J. McDonald, "Handbook of Biological Statistics," Sparky House Publishing, Baltimore, MD, 2009.